Theory of the extended x-ray-absorption fine structure*

Edward A. Stern
Department of Physics, University of Washington, Seattle, Washington 98195
(Received 14 March 1974)

A general theory of the fine structure observed on the high-energy side of the K-absorption edge (EXAFS) is presented. The form of the theory presented is useful when the excited atom is not too highly ionized and the potential is approximately spherically symmetric. A critical analysis is made of long-range-order theories of EXAFS and it is shown that the coherent effects of the periodic potential are not the dominant mechanism as assumed previously. The dominant mechanism is the scattering in the vicinity of the absorbing atom, and can most naturally be calculated by considering only the immediate environment surrounding the absorbing atom. Fourier-transforming EXAFS data determines the spatial dependence of a scattering matrix. This scattering matrix is expected to peak at the location of surrounding atoms, locating them, and can give information on the type of surrounding atoms and possibly the surrounding valence electron density. Because the K edges of different atoms are separated, such information can be obtained around each atom type separately, making EXAFS a potentially powerful tool for determining the microscopic structure of condensed matter.

I. INTRODUCTION

X radiation in passing through matter is absorbed, among other ways, by a photoelectric process—the direct excitation of the occupied-core electrons to unoccupied levels.[1] In this paper we will be concerned with the K-shell excitations which have a characteristic K edge for the onset of absorptions. X rays of energy below this edge are not absorbed by this mechanism while absorption by this mechanism can occur for energies above the K edge. Typically, as shown in Fig. 1, the absorption coefficient rises sharply at the K edge and then varies in a complicated fashion for energies somewhat above the edge, decreasing monotonically for energies more than a keV above the edge.[2,3] We are interested in the complicated variation of the absorption coefficient within an energy range of about 30 to about 1000 eV above the edge. There is further interesting structure in the first 30 eV above the edge where many-body interactions,[4] the distortion of the excited-state wave function by the Coulomb field of the excited atom,[5] and band effects all are important.[6] We will not attempt to understand this low-energy structure in this paper. To distinguish between the fine structure in the absorption coefficient below 30 eV to that above 30 eV, the fine structure above 30 eV is called the extended x-ray absorption fine structure (EXAFS).[7]

This paper is the first of three. The second paper[8] describes the experimental techniques used to measure EXAFS while the third paper[9] describes the data-analysis technique used to analyze the EXAFS measurements.

The first attempt to understand theoretically the EXAFS occurred about 40 years ago.[10] Since then there have been various further attempts to theoretically understand the EXAFS, but without complete success.[11-15] The various theories can be classified into two categories, long-range order (LRO) and short-range order (SRO). The LRO theories require the existence of long-range order to explain the fine structure. Because EXAFS is found experimentally in amorphous solids and molecules the experimental evidence favors the SRO theoretical approach. For this reason recent theoretical interest has centered on the SRO theories. In these theories only the evironment in the vicinity of the excited atom is held responsible for EXAFS. Most SRO theories of EXAFS agree on the basic physics. The differences occur in the various approximations made in the calculations.

However, there has never been detailed theoretical investigation of the relationship between the LRO and SRO theories although one knows that both approaches must give the same result if correctly formulated. This aspect is investigated in Sec. II where it is shown that the LRO theories as usually

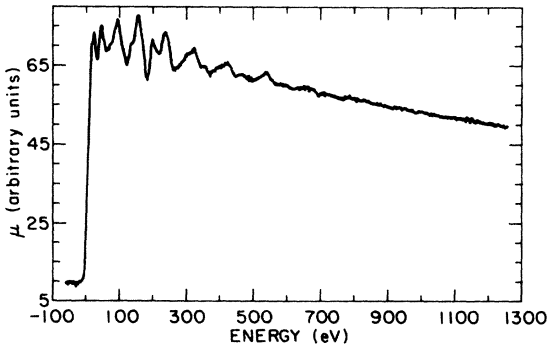

FIG. 1. K-shell mass absorption coefficient μ of copper plotted versus the photon energy of the x ray. The zero of energy is chosen at the K edge.

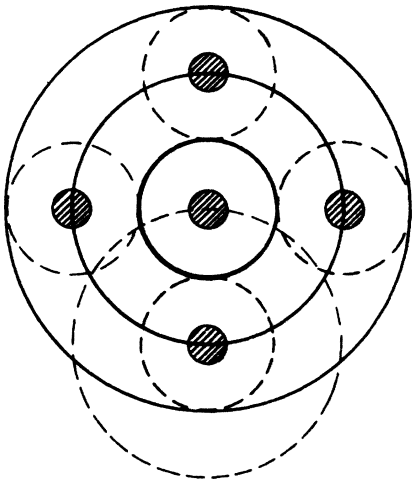

FIG. 2. Schematic picture of the excited electron wave function. The hatched circles represent the positions of atoms. The excited electronic state is centered about the center atom. The solid circles represent the crests of the outgoing part of the electron state. The surrounding atoms diffract the outgoing part as shown by the dotted circles.

formulated are incorrect because they neglect the dominant effects.

The probability of absorption of x rays by the K shell is given in the dipole approximation by[16]

$$W=\frac{2\pi^2e^2}{\omega c^2m^2}\,|M_{fs}|^2\,\rho(E_f)\ , \tag{1}$$

where

$$M_{fs}=\langle f|\vec{\mathrm{p}}\cdot\vec{\epsilon}|s\rangle\ .$$

Here $|s\rangle$ is the K-shell s state, $|f\rangle$ is the final unoccupied state of p symmetry, $\rho(E_f)$ is the density of states per unit energy at the energy of the final state E_f, ω is the frequency of the x ray, $\vec{\mathrm{p}}$ is the momentum operator, and $\vec{\epsilon}$ is the electric field vector of the x ray. In most SRO theories the $\rho(E_f)$ is assumed to be that of a free electron of energy $\hbar^2k^2/2m=E_f-E_0$, where E_0 is the zero of energy corresponding to the energy of $k=0$ free electrons. The value of E_0 is the effective average potential felt by an excited electron also called the "inner potential." The justification of the free-electron assumption for $\rho(E_f)$ is that for 30 eV or more above the Fermi level, the band effects will be small and negligible. With this assumption for $\rho(E_f)$, the only remaining factor that can contribute to the EXAFS is M_{fs}. The initial state $|s\rangle$ is fixed and does not vary with ω. The final state $|f\rangle$, however, does change with ω and produces the fine structure.[17]

To understand the mechanism that causes variations in $|f\rangle$ consider Fig. 2. The wave function $|f\rangle$ can be considered as a sum of two parts. If there were no atoms surrounding the excited atom the excited photoelectron would be in a solely outgoing state from the center atom as shown schematically as the outgoing solid lines. In this case M_{fs} would not show any fine structure and the x-ray absorption coefficient would vary monotonically with ω. This is the case for a single atom.[18] If now the excited atom is surrounded by other atoms as in a solid or molecule, the outgoing state scatters from the surrounding atoms producing ingoing waves shown in Fig. 2 as the dotted lines. These ingoing waves can constructively or destructively interfere with the outgoing wave near the origin where $|s\rangle$ exists. This interference causes an oscillatory behavior in M_{fs} as ω is varied, changing the electron wavelength and thus the phase between the ingoing and outgoing waves. Constructive interference increases M_{fs} while destructive interference decreases M_{fs} from what it would be if the excited atom were isolated.

The next significant step occurred when it was realized that an appropriate Fourier analysis of the EXAFS data can locate the positions of the atoms surrounding the x-ray absorbing atom.[19] This was important because it changed EXAFS from a qualitative effect to a quantitative one. It was shown, for example, that EXAFS could be used to determine the structure of amorphous solids and complex materials.[19] For studying the structure of materials EXAFS has an unique advantage over more standard methods such as x-ray diffraction because one can directly determine the location of atoms surrounding *each* constituent separately. The absorption edge of each constituent occurs at different energies and can be measured and Fourier transformed separately.

Another important aspect of the Fourier transform of EXAFS data is that this permitted, for the first time, an accurate comparison between theory and experiment. The previous manner for comparison between theory and experiment was qualitative—by comparing theoretical curves with experimental ones or by comparing peak positions.[3] These comparisons were done only qualitatively without any means to quantitatively evaluate the agreement. After Fourier analyzing the data one obtains peaks centered about the positions of the surrounding atoms.[9] The area under the peaks, their phases in respect to one another, and their location in real space can be compared with known crystal structures and the predictions of the theory. Details of how this comparison has been made will be given in Ref. 9. Suffice it to say that when this quantitative comparison was made, no known theory of the EXAFS could fit all details of the data. The Fourier transform had peaks centered about the positions of the surrounding atoms as predicted,

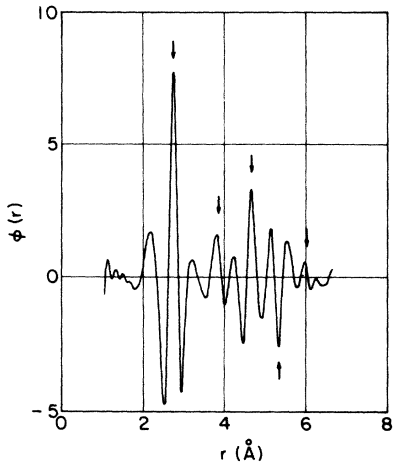

FIG. 3. Fourier transform of EXAFS data of crystalline copper plotted versus distance from the excited atom. The location of shells of atoms is shown by the arrows. Note that the fourth arrow from the left coincides with a peak of opposite sign from that of the other arrows.

but for copper the phases of the peaks changed sign as a function of the distance from the origin while the areas under the peaks had an unusual distance dependence. A change of sign of the phase of the peak means that the peak maximum has the opposite sign. Figure 3 shown a Fourier transform of crystalline copper EXAFS data. The peaks corresponding to the different atomic shells are indicated by the arrows. For comparison, the corresponding Fourier transform of crystalline germanium as shown in Fig. 4. Details of how these transforms were performed and a more detailed analysis of them is given in Ref. 9. For our purposes it suffices to focus on the relative phases of the peaks in crystalline Cu and Ge. We note that the fourth peak in copper is of opposite phase from the first three peaks while in Ge all of the peaks have the same phase.[20,21]

This change in phase cannot be explained by any past theories, though some recent ones[22,23] have been more promising. To understand why, we look at the best basic model used by the past theories. This model starts with an isolated atom as the zero-order system. Such an atom would have a sharp rise in x-ray absorption at the absorption edge and then a monotonically decreasing absorption coefficient as the energy of the x ray is increased. To obtain the fine structure one adds the perturbation of M_{fs} in Eq. (1) induced by the surrounding atoms as discussed above. If one has a single-component material, and multiple scattering effects are neglected, the scattering from each surrounding atom is approximately the same, at least for large k. In terms of the Fourier transforms of Figs. 3 and 4, this equality of scattering translates into a common phase and shape for the contribution of each shell of atoms. The magnitude of the contribution does vary depending on the number of atoms in each shell and the distance to the shell but the phase and shape is the same for each shell in this model. Clearly the data in Fig. 3 disagree with this prediction and the model is inadequate. To understand the experimental data in Fig. 3, one is forced to conclude that the scattering from the surrounding atoms are not all similar but must somehow vary, changing phase.

The critique of the past theories is that they do not adequately account for multiple scattering effects nor do they correctly take into account the fields induced by the absorbing atom. The absorbing atom is ionized by the x-ray photon and distortion of both the excited electron state and the surrounding atoms by the Coulomb potential of the absorbing atom occurs. Past calculations did not adequately account for both multiple scattering or Coulomb-field effects. Lee's calculation[22] suggests that multiple scattering effects may produce the observed change in phase for Cu. The importance of Coulomb effects has not been fully evaluated as yet.

In this paper we present a somewhat general formulation of EXAFS from which previously derived limits can be obtained. This formulation permits a more general perspective which shows that the Fourier transform of EXAFS measurements gives the spatial dependence of a scattering matrix which can be related, in a special case, to the electron charge density.

In Sec. II EXAFS is calculated for a simple pe-

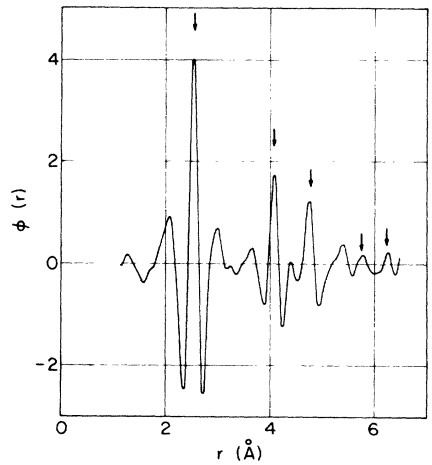

FIG. 4. Fourier transform of EXAFS data of crystalline Ge plotted versus distance from the excited atom. The location of shells of atoms is indicated by the arrows. In this case all peaks coinciding with the arrows have the same sign.

riodic solid to first order in the potential using a LRO theory. It is shown that previous LRO theories were in error. Section III presents a general formulation of EXAFS where it is shown that the Fourier transform of the experimental data gives the detailed spatial dependence around the excited atom of a scattering matrix. Various special cases for the scattering matrix are considered. Section IV consists of a discussion of the validity of various approximations made in the previous calculations. Section V consists of a summary and discussion.

II. SIMPLE PERIODIC SOLID

In this section we consider the problem of EXAFS in a periodic lattice which can be treated by the nearly-free-electron model. This is similar to the model first considered by Kronig[10] who treated the LRO in the two-wave approximation and is the prototype of other LRO calculations of EXAFS.

Krogin assumed that the changes in absorption occur because of changes in the density of final states, and not to changes in matrix elements as discussed in Sec. I. We proceed to show that the Kronig mechanism is not able to explain EXAFS, even if it is corrected for the matrix-element changes which are, as we will show, more important than density-of-state variations.

We are interested in treating all effects of first order in the potential so that it is necessary to assume that all Fourier components of the potential are very small. If we expand the periodic potential into its Fourier components then

$$V(\vec{r}) = \sum_{\vec{g}} V_g e^{i\vec{g}\cdot\vec{r}} , \tag{2}$$

where all $|V_{\vec{g}}|$ are small. Here $\vec{g}$ are the reciprocal-lattice vectors of the solid. In the two-wave approximation these $V_{\vec{g}}$ introduce gaps into the free-electron energy spectrum at values of $\vec{k} = \frac{1}{2}\vec{g}$. These gaps distort the density of states $\rho(E)$ from the free electron in a manner schematically shown in Fig. 6 by the dotted curve as first shown by Kronig.[10] The amount of the enhancement of $\rho(E)$ is proportional to V_g while the width of the region enhanced is also proportional to V_g.

From Fig. 1 note that the period of the EXAFS is of the order of 50 eV. The experimental resolution used in the measurement[8] illustrated in Fig. 1 is of the order of 10 eV. Both these energies are large compared to what V_g can be and still allow the nearly-free-electron model to be valid, at least for electron energies less than 100 eV. For the sake of definitiveness it is assumed that $V_g \ll 10$ eV. In that case the structure introduced by $\rho(E)$ is much sharper than the experimental resolution and can be approximated by a δ function whose coefficient is proportional to the change in area introduced by the structure. The total change in area is zero because the total number of states remains the same as one integrates over the structure. Even if one introduces a δ function separately for each peak of the structure, the area of each peak is of order V_g^2 which is negligible since only order V_g is to be kept. Thus the Kronig mechanism cannot explain EXAFS, in agreement with the experimental indications.[3]

The Kronig mechanism neglects a very important, in fact the dominant, effect, namely, the change in matrix element referred to in Sec. I. The periodic potential introduces a major change in the electron states in addition to changes in $\rho(E)$. If the potential has a center of symmetry, electron states that satisfy the condition for Bragg scattering, namely

$$\vec{k}\cdot\vec{g} = \tfrac{1}{2}g^2 , \tag{3}$$

are changed from $e^{i\vec{k}\cdot\vec{r}}$ to $e^{i\vec{k}_\perp\cdot\vec{r}}$ ($\sin\frac{1}{2}\vec{g}\cdot\vec{r}$ or $\cos\frac{1}{2}\vec{g}\cdot\vec{r}$), where $\vec{k}_\perp$ is the component of $\vec{k}$ perpendicular to $\vec{g}$. The sine or cosine function is the eigenstate either just below or just above the gap. If the potential V_g is attractive then the eigenstate just below the gap is the cosine function.

If we are interested in the K-absorption edge, the initial state in the matrix element of Eq. (1) has s symmetry and its matrix element with the cosine function is zero while its matrix element with the sine function is $\sqrt{2}$ times larger than for a plane wave, taking into account the normalization of the wave function. Thus there are large matrix-element variations which were neglected by Kronig.

We can include these matrix-element effects with sufficient accuracy for an order-of-magnitude estimate as follows. For the sake of definitiveness, assume an attractive V_g so that the state just below the gap has the cosine term. Referring to Fig. 5, consider a constant k surface which intersects the energy region within V_g from the zone face. The zone faces are denoted by the solid vertical lines while the dotted lines enclose the energy region within V_g of the zone face. The states within the energy region V_g below the zone face, having the cosine form, contribute approximately zero to the absorption in Eq. (1) while those within the energy range V_g above the zone face, having the sine form, contribute approximately twice as much to the absorption as do the unperturbed states. As the radius of the constant k surface is increased from small values to pass through the zone face, the absorption within the dotted region of width of order $2V_g$ is appreciably affected by the zone face. For values of k between dotted planes 1 and the $\frac{1}{2}g$ planes, the matrix element is decreased, while for values of k between the $\frac{1}{2}g$ planes and the dotted

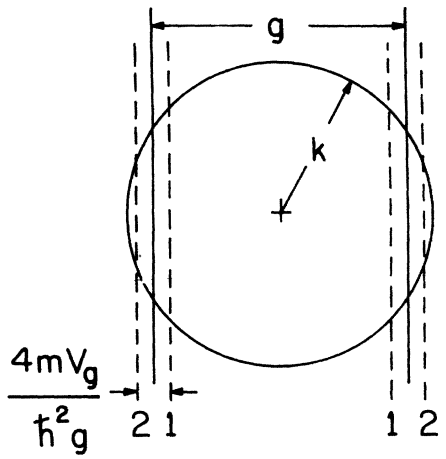

FIG. 5. Sphere of radius k plotted in k space. The Brillouin-zone planes corresponding to the reciprocal vector $\vec{g}$ are plotted as the solid lines. Planes 1 and 2 shown by the dotted lines enclose the region where the periodic potential greatly affects the form of the wave function.

planes 2, the matrix element is enhanced. For magnitudes of k less than $\frac{1}{2}g$, the matrix element is only decreased by the periodic potential when k is large enough to cross the dotted planes 1. When k is greater than $\frac{1}{2}g$, the matrix element is decreased for some states and increased for others. The number of states decreased is equal to those enclosed between planes 1 and the $\frac{1}{2}g$ planes. This number is proportional to the distance between these two planes, namely, $2mV_g/\hbar^2 g$. The number of states with increased matrix elements is equal to those enclosed between the $\frac{1}{2}g$ planes and the planes 2. The number of such increased states is proportional to either $k-\frac{1}{2}g$ if the sphere does not intersect the planes 2, or the distance between the $\frac{1}{2}g$ planes and the planes 2, namely $2mV_g/\hbar^2 g$, if the sphere does intersect the planes 2. When the sphere does intersect the planes 2, the enhanced states just compensate the decreased states and the total absorption is at the free-electron value. For values of k such that planes 1 are intersected but planes 2 are not, the total absorption is decreased below the free-electron value. The expected behavior is shown schematically in Fig. 6.

Replacing this structure by a δ function as before, it is noted that the matrix element contributes a nonzero area so that it is more important than the $\rho(E)$ variation. However, the area is proportional to V_g^2 and is thus still negligible. Thus, no significant contribution to the EXAFS comes from the vicinity of the zone boundaries so that the LRO theories which are based on this mechanism are incorrect.

It was reasoning based on this incorrect LRO-theory mechanism that led to the conclusion that the periodic potential is not the cause of EXAFS and that EXAFS is caused exclusively by the perturbation introduced by the excited hole which perturbs the periodic potential.[21] However, this conclusion neglected the mechanism missing in the LRO theory of Kronig. The correct result is that both the periodic potential and the perturbation introduced by the excited hole must be included. As indicated before, only of order V_g of the states are strongly modified by the zone boundary. The missing mechanism comes from the rest of the states which are only weakly modified by the V_g, and their contributions can be treated by perturbation theory. For first order in V_g, the wave function is

$$\psi_k = e^{i\vec{k}\cdot\vec{r}} + \sum_{\vec{g}} V_{\vec{g}} \frac{e^{i(\vec{k}+\vec{g})\cdot\vec{r}}}{E_{\vec{k}} - E_{\vec{k}+\vec{g}}}, \tag{4}$$

where $E_{\vec{k}} = \hbar^2 k^2/2m$. This perturbation of the wave function modifies the absorption to order V_g for a given state. Since practically all of the states are so affected at a given energy, the change in absorption at a given energy is always of order V_g. Thus this mechanism dominates over the Kronig one.

An important conclusion from this result is that the coherent effects introduced by the long-range order, which must be treated to infinite order in V_g, are not important and can be neglected. The EXAFS can be calculated by treating a weak potential to only first order, i.e., in the Born approximation. Since the x-ray photon causes a transition from a core state which is localized on a single atom, the most natural frame in which to calculate the transition is one centered about this absorbing

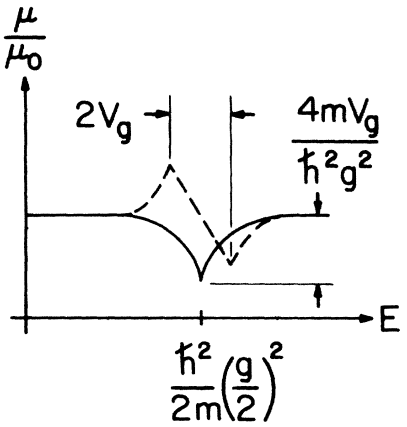

FIG. 6. Sketch of the ratio of the K-shell mass absorption coefficient in the nearly-free-electron model μ versus energy of the excited electron. The dotted curve is the contribution of the density-of-states changes while the solid curve is the contribution of the large change in matrix element near the Brillouin-zone face.

atom. This is just the SRO approach and our discussion justifies the advantage of this approach. In Sec. III we will use the SRO approach to obtain some general results for EXAFS.

III. GENERAL FORMULATION

It is assumed that the system to be studied can be treated by a single-particle Hamiltonian. Many-body effects such as shielding are included in the single-particle potential as much as possible. The lifetime introduced by electron-electron scattering can be accounted for in the potential by permitting it to be complex. The Hamiltonian of the system before absorption is

$$H_1 = p^2/2m + V_1(\vec{r}) + V_0(\vec{r}) \ , \tag{5}$$

and after absorption is

$$H_2 = p^2/2m + V_2(\vec{r}) + V_0'(\vec{r}) \ . \tag{6}$$

Here $V_0(r)$ and $V_0'(r)$ are the potentials contributed by the atom before and after absorbing an x-ray photon, respectively. $V_1(\vec{r})$ and $V_2(\vec{r})$ are the potentials contributed by the surrounding environment before and after the absorption, respectively, and can differ from one another because of perturbations induced via the ionized hole a la a Stark-like effect. The region in which V_1 and V_2 differ significantly is localized around the origin. Some questions have been raised whether V_2 and V_0' should be the potentials where the positive excited hole is completely screened or unscreened. If the lifetime of the excited state is long compared to the time it takes for the screening charge to relax around the hole, then the screened potential should be used. If the lifetime of the excited state is short compared to this relaxation time, then the unscreened potential should be used. In the intermediate lifetime case, neither V_0' nor V_2 can be approximated by a static potential. It is assumed for our discussion that both V_0' and V_2 can be approximated by a static potential.

The initial state is a K-shell electron whose solution is an atomic problem which is assumed known. The final excited state is one which propagates outwardly from the excited atom. This state must have p symmetry in its outward-going part in order to have absorption when the atom is isolated. Then the atom is placed in condensed matter, the excited state is modified, mixing in other symmetries besides p type. Only the p-character part will contribute to the absorption and the modification in it introduced by the condensed-matter environment will produce changes in absorption via interference effects. Other states which don't start out with p symmetry in the isolated atom will have some p character mixed in by the condensed-matter environment. However, the change in absorption for these states does not show interference effects. For EXAFS we are interested in only the interference term, and the appropriate excited state to consider is one that initially propagates outward with p character.

The excited state will be calculated from the integral solution of the Hamiltonian in (6),

$$\psi = \psi_k + G_0 V_2' \psi \ . \tag{7}$$

Here ψ_k is the solution of the equation

$$\begin{aligned} &H_0\psi_k = E\psi_k \ , \\ &V_2'(r) = V_2(r) - E(k) \ , \\ &H_0 = p^2/2m + V_0'(r) + E(k) \ , \end{aligned} \tag{8}$$

and $E(k)$ is the "inner potential" contributed by $V_2(r)$. For weak potential $E(k)$ is the value of $V_2(r)$ averaged over $|\psi_k(r)|^2$. For stronger potentials it is the average value of a scattering matrix T to be defined below. It is assumed that at the energies of interest for EXAFS, $E(k)$ is a function only of the magnitude of k and not its direction. The wave number k is defined by

$$\hbar^2k^2/2m = E - E(k) \ . \tag{9}$$

The "inner potential" $E(k)$ is the contribution of $V_2(\vec{r})$ to the potential "zero," above which the "kinetic energy" given in (9) is added to determine the total energy of the ψ_k state.

In this section the potential of the excited atom $V_0'(r)$ is assumed to be spherically symmetric and short ranged. Relaxation of this restriction will be discussed in Sec. IV. A solution of (8) corresponding to an outgoing p wave from the origin can be written

$$\psi_k^+(r) = U_k(r)(z/r) \ . \tag{10}$$

The results for the other two p waves varying as x and y are easily obtained from the results of considering the form of (10), so that we first focus on the presence of just the ψ_k^+ given in (10).

When $r > r_c$, where r_c is the radius outside of which $V_0'(r)$ is negligible, ψ_k^+ can be written in the form

$$\psi_k^+ = B e^{i\delta_1} h_1^+(kr)(z/r) \ ,$$

where B is a normalization constant, and

$$h_1^+(x) = e^{ix}\left(\frac{1}{x} + \frac{i}{x^2}\right) \tag{11}$$

is the outgoing spherical Hankel function. The phase shift δ_1 is introduced by the potential V_0' of the excited atom.

It is convenient to define a scattering matrix by the relation

$$T\psi_k^+ = V_2'\psi \ , \tag{12}$$

so that (7) becomes

$$\psi = \psi_k^+ + \psi_{sc} , \tag{13}$$

where

$$\psi_{sc} = G_0 T \psi_k^+ . \tag{14}$$

As mentioned previously, only the part of ψ_{sc} that has p symmetry near the origin is of interest for EXAFS. Using a form of G_0 expanded in spherical harmonics about the origin,[24] the p part of ψ_{sc} near the origin is given by

$$\psi'_{sc} = \frac{i3mkz}{8\pi^2\hbar^2 r} U_k^-(r) I_z(k) ,$$

where

$$I_z(k) = \int \psi_k^+(\vec{r}') T(\vec{r}', \vec{r}'') \psi_k^+(\vec{r}'') d^3r' d^3r'' . \tag{15}$$

$U_k^-(r)$ is the regular solution of (8) and near the origin has exactly the same form as ψ_k^+. To calculate the matrix element in (1) it is sufficient to know ψ'_{sc} near the origin within the core region where the initial K-shell wave function is finite. In this same region $U_k^-(r)$ and ψ_k^+ have the same r dependence and the matrix element M_{fs} in (1) becomes

$$M_{fs}^z = M_{fs}^{0z}\left(1 + \frac{3imk}{8\pi^2\hbar^2} I_z(k)\right) , \tag{16}$$

where M_{fs}^{0z} is the matrix element with $T = 0$, and varies monotonically with energy above the edge. Since we are neglecting variations in $\rho(E)$ caused by $V_2(r)$, the probability of absorption as given in (1) becomes, using (16),

$$W_z = W_{0z}\left(1 - \frac{3mk}{4\pi^2\hbar^2} \mathrm{Im} I_z(k) + \frac{9}{16} \frac{m^2k^2}{(2\pi^2\hbar^2)^2} |I_z(k)|^2\right) , \tag{17}$$

where W_{0z} is the absorption when $T = 0$ and is monotonically varying above the absorption edge.

Transitions are also possible to final states ψ_k^+ with p symmetry varying as x and y in addition to the assumed z variation. Adding their contributions, the total absorption is given by

$$W = W_0\left[1 - \frac{3mk}{4\pi^2\hbar^2} \mathrm{Im} \sum_\alpha |\vec{e}\cdot\hat{\alpha}|^2 I_\alpha(\vec{k}) \frac{+9m^2k^2}{16(2\pi^2\hbar^2)^2} \sum_\alpha |I_\alpha(k)|^2 |\vec{e}\cdot\hat{\alpha}|^2\right] , \tag{18}$$

where α can be x, y, or z, $\vec{e}$ is a unit vector in the direction of the polarization of the x-ray photon, $\hat{\alpha}$ is a unit vector in the α direction, and

$$I_\alpha = \int U_k(r') \frac{\alpha'}{r'} T_k(\vec{r}', \vec{r}'') U_k(r'') \frac{\alpha''}{r''} d^3r' d^3r'' . \tag{19}$$

The oscillatory behavior of EXAFS comes from the middle interference term on the right-hand side of (18). The last term in (18) will vary smoothly with k. By analysis of the experimental data it is possible to separate out the smoothly varying terms from the oscillatory terms[9] and determine the quantity $\chi(k)$ defined by

$$\chi(k) = \frac{3mk}{4\pi^2\hbar^2} \mathrm{Im} \sum_\alpha I_\alpha(k) |\vec{e}\cdot\hat{\alpha}|^2 . \tag{20}$$

The function $\chi(k)$ has much detailed information about the microscopic environment surrounding the absorbing atom which can be obtained by Fourier transforming it.[19] To illustrate this, consider several special cases for T. First assume that T is localized around sites $\vec{R}_n$ so that

$$T_k(\vec{r}', \vec{r}'') = \sum_n t_n(2k) \delta(\vec{r}' - \vec{R}_n) \delta(\vec{r}' - \vec{r}'') e^{-2r'/\lambda} . \tag{21}$$

The λ in the exponential is the mean-free path of the excited state due to electron-electron scattering, and $t_n(2k)$ is assumed to be real. Then $\chi(k)$ of (20) becomes

$$\chi_1(k) = \frac{3mk}{4\pi^2\hbar^2} \mathrm{Im} \sum_\alpha I_{1\alpha}(k) |\vec{e}\cdot\hat{\alpha}|^2 , \tag{22}$$

where

$$I_{1\alpha}(k) = \sum_n t_n(2k) e^{2i(kR_n + \delta_1)} e^{-2R_n/\lambda} \times \left(\frac{1}{kR_n} + \frac{i}{(kR_n)^2}\right)^2 \left(\frac{\alpha_n}{R_n}\right)^2$$

and α_n is the αth component of $\vec{R}_n$.

Consider the Fourier transform of $k\chi_1(k)$,

$$F_1(r) = \frac{3m}{4\pi^2\hbar^2} \int_0^\infty \sum_\alpha \mathrm{Im} I_{1\alpha}(k) \times e^{-2i(kr + \delta_1)} k^2 \frac{dk}{2\pi} |\vec{e}\cdot\hat{\alpha}|^2 . \tag{23}$$

The phase shift δ_1 is included in the Fourier-transforming exponential to cancel the one in $I_1(k)$ and simplify the final expressions. This phase shift is k dependent and unknown. In practice the actual transform is taken with $\delta_1 = 0$: The modification of the final result in the actual case is not changed in its essential character from the result presented here. More details are given in Ref. 9.

For values of $kR_n \gg 1$,

$$F_1(r) \approx F_1^0(r) = \frac{3im}{8\pi^2\hbar^2} \sum_{n,\alpha} \frac{t_n(-r - R_n) - t_n(R_n - r)}{R_n^2}$$

$$\times e^{-2R_n/\lambda}\left(\frac{\alpha_n}{R_n}\right)^2 |\vec{e}\cdot\hat{\alpha}|^2 ,$$

where

$$t_n(x) = \int_0^\infty t_n(2k) e^{2ikx} \frac{dk}{2\pi} .$$

In our model $t_n(x)$ is localized around $x = 0$, and since $r > 0$, we can then neglect $t_n(-r - R_n)$ to obtain

$$F_1^0(r) = \frac{-3im}{8\pi^2\hbar^2} \sum_{n,\alpha} \frac{t_n(R_n - r)}{R_n^2} \times e^{-2R_n/\lambda}\left(\frac{\alpha_n}{R_n}\right)^2 |\vec{e}\cdot\hat{\alpha}|^2 . \quad (24)$$

More exactly, if kR_n is not assumed to be much greater than 1, which it won't be for small k, $F_1(r)$ satisfies the relation

$$-4\int k^3\chi(k) e^{-2i(kr+\delta_1)} \frac{dk}{2\pi} = \frac{d^2F_1(r)}{dr^2} = \frac{-3im}{8\pi^2\hbar^2} \sum_{n,\alpha} \frac{e^{-2R_n/\lambda}}{R_n^2}\left(\frac{\alpha_n}{R_n}\right)^2 |\vec{e}\cdot\hat{\alpha}|^2 \times\left(\frac{d}{dr} + \frac{2}{R_n}\right)^2 t_n(R_n - r) , \quad (25)$$

where

$$\left(\frac{d}{dr} + \frac{2}{R_n}\right)^2 \equiv \left(\frac{d^2}{dr^2} + \frac{4}{R_n}\frac{d}{dr} + \frac{4}{R_n^2}\right) .$$

In a realistic situation, R_n in a given shell will not be the same about every atom at a given instant of time but will have a probability distribution $P(R_n)$ due to thermal vibrations or disorder. Since the experimental data average the absorption over many atoms, analysis of EXAFS will lead to $\langle F_1(r)\rangle$ where

$$\frac{d^2\langle F_1(r)\rangle}{dr^2} = \frac{-i3m}{8\pi^2\hbar^2} \sum_{n,\alpha} |\vec{e}\cdot\hat{\alpha}|^2 \int P(R_n)\, dR_n \times \frac{e^{-2R_n/\lambda}}{R_n^2}\left(\frac{\alpha_n}{R_n}\right)^2 \left(\frac{d}{dr} + \frac{2}{R_n}\right)^2 t_n(R_n - r) . \quad (26)$$

If the medium, after averaging, has cubic or higher symmetry, or is polycrystalline or if the incoming x-ray photons are unpolarized, (26) simplifies to

$$Q_1(r) \equiv \frac{d^2\langle F_1(r)\rangle}{dr^2} = \frac{im}{8\pi^2\hbar^2} \sum_n \int P(R_n)\, dR_n \times \frac{e^{-2R_n/\lambda}}{R_n^2}\left(\frac{d}{dr} + \frac{2}{R_n}\right)^2 t_n(R_n - r) . \quad (27)$$

The Eqs. (22)–(27) generalize the results which have been presented previously.[15,19,21] From (27), since t_n is localized around R_n, the function $Q_1(r)$ is localized around the atoms surrounding the absorbing atom and thus $Q_1(r)$ can be used to determine the position of neighboring atoms.[9] By observing EXAFS above the absorption edge of each component, the local environment about each component can separately be obtained and there is no need to use single crystals to do so.

Now assume that V_2' is weak so that

$$T(\vec{r}', \vec{r}'') = V(\vec{r}')\delta(\vec{r}' - \vec{r}'') . \quad (28)$$

$V(\vec{r})$ is the potential of the surrounding atoms modified by the ionized hole at the origin. Then the Fourier transform of $-4k^3\chi(k)$ in this case becomes

$$-\int 4k^3\chi(k) e^{-2i(kr+\delta_1)} \frac{dk}{2\pi} = \frac{d^2F_2(r)}{dr^2} = -\frac{3m}{32\pi^2\hbar^2}\left[i\left(\frac{\partial}{\partial r} + \frac{2}{r}\right)^2 \sum_\alpha A_\alpha(r) |\vec{e}\cdot\hat{\alpha}|^2 + \frac{P}{\pi}\int\left(\frac{\partial}{\partial r} + \frac{2}{r'}\right)^2 \sum_\alpha \frac{A_\alpha(r')}{r' - r} |\vec{e}\cdot\hat{\alpha}|^2 dr'\right] , \quad (29)$$

where P means the principal value of the integral is to be taken,

$$A_\alpha(r') = \int (\alpha'/r')^2 V(\vec{r}')\, d\Omega' ,$$

and $d\Omega'$ is a differential solid angle.

As before, experiment determines $\langle F_2(r)\rangle$ averaged over the various environments surrounding a given atom. If the medium, after averaging, has cubic or higher symmetry, or is polycrystalline, or if the incoming x-ray photons are unpolarized (29) simplifies to

$$Q_2(r) \equiv \frac{d^2\langle F_2(r)\rangle}{dr^2} = \frac{-m}{32\pi^2\hbar^2}\left[i\left(\frac{\partial}{\partial r} + \frac{2}{r}\right)^2 \langle A(r)\rangle + \frac{P}{\pi}\int\left(\frac{\partial}{\partial r} + \frac{2}{r'}\right)^2 \frac{\langle A(r')\rangle}{r' - r} dr'\right] , \quad (30)$$

where

$$\langle A(r)\rangle = \int \langle V(\vec{r})\rangle\, d\Omega .$$

Note from (30) that the Fourier transform of EXAFS data when $V(r)$ is weak can determine $\langle A(r)\rangle$, the integral over solid angle of the potential at r. In this case, the charge density integrated over solid angle $\langle q(r)\rangle$ can also be determined by calculating

$$\frac{1}{r^2}\frac{\partial}{\partial r}r^2\frac{\partial}{\partial r}\langle A(r)\rangle = -4\pi\langle q(r)\rangle \ . \tag{31}$$

In the general case

$$\frac{d^2\langle F(r)\rangle}{dr^2} \equiv -4\int k^3\chi(k)e^{-2i(kr+\delta_1)}\frac{dk}{2\pi}$$

$$= -i\frac{3m}{8\pi^2\hbar^2}\sum_\alpha |\vec{e}\cdot\hat{\alpha}|^2\int\left(\frac{\partial}{\partial r}+\frac{2}{r'}\right)\left(\frac{\partial}{\partial r}+\frac{2}{r''}\right)\left\langle\sum_\alpha(r,r',r'')\right\rangle dr'\,dr'' \ , \tag{32}$$

where

$$\sum_\alpha(r,r',r'') = \int\langle S_k(\vec{r}',\vec{r}'')e^{i[k(r'+r''-2r)+\Delta_k(\vec{r}',\vec{r}'')]}\rangle\,\alpha'\alpha''\frac{dk}{2\pi}d\Omega'\,d\Omega'' \ ,$$

and

$$T_k(\vec{r}',\vec{r}'') = S_k(\vec{r}',\vec{r}'')e^{i\Delta_k(\vec{r}',\vec{r}'')} \ .$$

Both S_k and Δ_k are real and it is assumed, as before, that the Fourier transform over $e^{-ik(r'+r''+2r+2\delta_1)}$ is negligible. Again, if the medium, after averaging, has cubic or higher symmetry, or is polycrystalline, or if the incoming x-ray photons are unpolarized, (32) simplifies to

$$Q(r) = \frac{-im}{8\pi^2\hbar^2}\int\left(\frac{\partial}{\partial r}+\frac{2}{r'}\right)\left(\frac{\partial}{\partial r}+\frac{2}{r''}\right)\left\langle\sum(r,r',r'')\right\rangle dr'\,dr'' \ ,$$

where

$$\sum(r,r',r'') = \int\langle S_k(\vec{r}',\vec{r}'')e^{i[k(r'+r''-2r)+\Delta_k(\vec{r}',\vec{r}'')]}\rangle\,(\vec{r}'\cdot\vec{r}'')\frac{dk}{2\pi}d\Omega'\,d\Omega'' \ . \tag{33}$$

IV. DISCUSSION

The theory of EXAFS presented in Sec. III made several assumptions which we will evaluate in this section. One assumption was that beyond a distance $r > r_c$, the effect of the center atom can be accounted for by a phase shift δ_1. Although it was not explicitly assumed, for practical purposes it is useful if r_c is less than the first-nearest-neighbor distance so that the Fourier transform can accurately determine the location of all neighbors. Since the center atom in the excited state is positively charged, this assumption implies either that the Coulomb potential is shielded within a nearest-neighbor distance, or, if it is not, that it can be approximated by a phase shift. In metals one expects reasonably good shielding by the first neighbor distance and the assumption of a phase shift should be satisfactory.

In semiconductors and insulators, the Coulomb potential may not be completely shielded and Coulomb wave function must be used in place of spherical Hankel functions. The asymptotic form for Coulomb wave functions is[5]

$$R_{kl} \to (2/\pi)\sin[kr + (1/k)\ln 2kr + \tfrac{1}{2}l\pi + \delta_l] \ , \tag{34}$$

where

$$\delta_l = \arg\Gamma(l+1-i/k) \ .$$

k and r are expressed in atomic units and for p waves $l=1$. In the limit that $k \gg 1$, δ_l and the ln term become unimportant and the spherical Hankel-function approximation used in Sec III is valid. In terms of ordinary units the condition $k \gg 1$ is

$$k \gg Z/a_0 \ , \tag{35}$$

where a_0 is the Bohr radius for the hydrogen atom of about 0.5 Å and Z is the positive charge on the center atom. If the atom is initially neutral, then $Z=1$ and the condition for the neglect of Coulomb effects is

$$k \gg 2A^{-1} \ ,$$

or

$$E \gg 15 \text{ eV} \ , \quad Z=1 \ . \tag{36}$$

Condition (36) indicates that because of Coulomb effects the EXAFS theory of Sec. III is not valid in insulators and semiconductors till energies 50 or so eV above the edge. However, in this low-energy range the theory is also not valid because it neglects band effects on the density of states. One expects band effects to be important in this low-energy range, in general, and thus above about

50 eV where band effects can be neglected, Coulomb effects can also be neglected, if the atom is initially neutral.

However, there may be cases of ionic binding where the initial state is not neutral and thus Z can be larger than 1. If $Z=3$, then the condition for neglect of Coulomb effects is

$$E \gg 135 \text{ eV}, \quad Z=3. \tag{37}$$

In this case Coulomb effects are not negligible. The most prominent EXAFS structure occurs below 300 eV and thus would be appreciably affected by Coulomb effects if the initial bonding is ionic enough to transfer two electron charges. Thus for atoms in a highly ionic bonding state, the theory presented in Sec. III would not be applicable.

Another assumption made in Sec. III was that V_0', the potential of the central atom, is spherically symmetric. If the local environment is asymmetric enough it can invalidate this assumption, e.g., if the central atom has strong covalent or ionic bonding with a single neighbor and weaker bonding with other neighbors.

Although the theory presented in Sec. III formally includes multiple scattering effects by introducing T_k, in practice the usefulness of EXAFS depends on multiple scattering effects between neighboring atoms being weak enough so that there is a simple correlation between T_k and V_2', and thus the location of the atoms. Fortunately, at energies above 50 eV where band effects can be neglected, the scattering should be weak enough so that multiple scattering effects between atoms will not be too great. Numerical calculations by Lee[22] confirm this to be the case for Cu. He finds that multiple scattering is only important for those atoms which are shadowed from the outgoing wave by a nearer atom. Normally this shadowing does not occur till fourth or further neighbors.

The multiple scattering effects within an atom do not change the correlation between the location of an atom and where its scattering is localized in space, only multiple scattering between various atoms will do so. The first approximation given in Eqs. (21)–(27) can adequately handle the case where multiple scattering effects between atoms is small while multiple scattering effects within a given atom can be accounted for to all orders. The total phase shift in the scattered wave can have, in addition to the central atom contribution δ_1, additional contributions from the t_n of (21) which can be complex in general. Experimentally the relative importance of δ_1 and contributions from t_n can be determined by noting whether the total measured phase shift is dependent on only the type of central atom or the environment. Present experimental indications are that δ_1 dominates.[9]

Even if the neighboring atoms are all of the same type, t_n in (21) may be different in different neighboring shells. This difference can occur by multiple scattering effects between atoms, by the potential of the central ionized atom modifying the surrounding atoms by a Stark-like effect, or by the fact that the outgoing wave is spherical and the relative weight of different partial waves vary in the various neighboring shells. This latter effect becomes negligible for large enough kR_n. Numerical estimates[22] for Cu by Lee indicate that this latter effect is only significant for the first shell where the effect is still small and can be neglected without great error.

The second approximation in Sec. III where V_2' was assumed weak should be a good approximation for the valence electrons of the solid, and the discussion there indicated that the charge density can be determined from EXAFS in that case. If this turns out to be true in practice, EXAFS, then, would have the exciting potential of measuring the valence electron density in the vicinity of the central atom. In addition, t_n in (21) should be a signature of the type of atom at R_n. Thus, from the shape of $t_n(R_n - r)$ one may be able to distinguish the type of atom at R_n.

V. SUMMARY AND CONCLUSIONS

The inadequacy of previously proposed long-range theories to explain EXAFS is elucidated. A generalized theory of EXAFS is presented showing that an appropriate Fourier transform of the experimental data gives information on the scattering matrix as a function of position. In cases where multiple scattering effects between atoms are small, the Fourier transform can determine the radial location and types of surrounding atoms. With enough experimental resolution, the possibility of determining the valence charge density at distance r from the origin integrated over solid angle appears promising.

The feature of EXAFS that makes it particularly attractive is the ability to determine the environment around each type of atom separately. This occurs because the x-ray edges of many atoms are far enough separated in energy that their EXAFS do not overlap. Since EXAFS measures the immediate environment around a given type of atom, it does not require that the sample be single crystal or even crystalline. Thus amorphous, liquid, and other disordered states can be investigated in addition to crystalline forms. With polarized x rays and single crystals, anisotropic effects are measurable by EXAFS if the crystal symmetry is less than cubic. The greatest usefulness for EXAFS should be in measuring materials which are composed of many different types of atoms in a disordered form such as biological systems, amorphous solids, complicated alloys and compounds.

ACKNOWLEDGMENTS

Valuable and numerous discussions with Farrell Lytle and Dale Sayers are gratefully acknowledged. Important discussions with Patrick Lee, Sebastian Doniach, and Arthur Bienenstock are also gratefully acknowledged.

---

*Research supported in part by the Air Force Office of Scientific Research, Office of Aerospace Research, U.S.A.F.

[1]R. B. Leighton, *Principles of Modern Physics* (McGraw-Hill, New York, 1959), pp. 421–435.

[2]L. G. Parratt, Rev. Mod. Phys. 31, 616 (1959).

[3]L. V. Azaroff, Rev. Mod. Phys. 35, 1012 (1963).

[4]G. D. Mahan, Phys. Rev. 163, 612 (1967); 153, 882 (1967); J. J. Hopfield, Comments on Solid State Phys. 2, 40 (1969); M. Combescot and P. Nozières, J. Phys. 32, 913 (1971).

[5]L. D. Landau and E. M. Lifshitz, *Non-Relativistic Quantum Mechanics* (Addison-Wesley, Cambridge, Mass., 1958), pp. 121–127.

[6]D. A. Papaconstantopoulos, Phys. Rev. Lett. 31, 1050 (1973).

[7]F. W. Lytle, in *Physics of Non-Crystalline Solids*, edited by J. A. Prins (North-Holland, Amsterdam, 1965), pp. 12–25.

[8]F. W. Lytle and D. E. Sayers (unpublished).

[9]D. E. Sayers, E. A. Stern, and F. W. Lytle (unpublished).

[10]R. de L. Kronig, Z. Phys. 70, 317 (1931); 75, 191 (1932).

[11]H. Petersen, Z. Phys. 80, 258 (1933); D. R. Hartree, R. de L. Kronig, and H. Petersen, Physica 1, 895 (1934).

[12]A. I. Kostarev, Zh. Eksp. Teor. Fiz. 11, 60 (1941); 19, 413 (1949).

[13]T. Hayasi, Sci. Rep. Tôhoku Univ. 33, 123 (1949); 33, 183 (1949); 34, 185 (1950); 44, 87 (1960).

[14]T. Shiraiwa, T. Ishimura, and M. Sawada, J. Phys. Soc. Jpn. 13, 847 (1958); T. Shiraiwa, J. Phys. Soc. Jpn. 15, 240 (1960).

[15]A. I. Kozlenkov, Izv. Akad. Nauk SSSR 25, 957 (1961) [Bull. Acad. Sci. USSR Phys. Ser. 25, 968 (1961)]; D. E. Sayers, F. W. Lytle, and E. A. Stern, in *Advances in X-ray Analysis*, edited by B. L. Henke, J. B. Newkirk, and G. R. Mallett (Plenum, New York, 1970), Vol. 13, p. 248.

[16]H. Bethe and E. Salpeter, *Quantum Mechanics of One and Two Electron Systems* (Springer-Verlag, Berlin, 1957), Secs. 59 and 69.

[17]The idea of the change in wave function of the final state by interference appears to have been first clearly used by the second reference of Ref. 11.

[18]A. E. Sandström, *Handbuch der Physik* (Springer-Verlag, Berlin, 1957), Vol. 30, p. 211. The absorption for an isolated atom can also have a nonmonotonic variation due to virtual resonant states but such effects are important only near the edge, say within 50 eV or so.

[19]D. E. Sayers, E. A. Stern, and F. W. Lytle, Phys. Rev. Lett. 27, 1204 (1971).

[20]The data for Cu are different from that given previously in Ref. 21 because of an error in the computer program used in obtaining the Fourier transform of the data.

[21]E. A. Stern and D. E. Sayers, Phys. Rev. Lett. 30, 174 (1973).

[22]P. Lee (unpublished).

[23]C. Ashley and S. Doniach (unpublished).

[24]L. S. Rodberg and R. M. Thaler, *Introduction to the Quantum Theory of Scattering* (Academic, New York, 1967), p. 118.